EXTERNAL-JET (FLUID) PROPULSION
ANALOGY FOR PHOTONIC (LASER) PROPULSION

By John R. Cipolla, Copyright February 21, 2017

ABSTRACT

External-jet propulsion uses a narrow jet of high velocity water or conceptually a bank of high power lasers[1] to "blast" vehicles to high velocity. The original goal of this work was

to create a design analogy for launching micro-sized laser-propelled probes to 20 percent of the speed of light to the nearest stars. This work also resulted in the practical capability to launch micro-craft on external jets of high velocity water having a mass of only 0.7 grams, which represents the smallest known reusable jet propelled vehicle in history. A sphere-cone projectile having a hollow interior shaped like a diverging nozzle demonstrated the concept of propelling projectiles to high velocity using the principal of conservation of linear momentum[2, 8]. An extremely narrow streamtube of high velocity water directed into the interior of a sphere-cone successfully demonstrated stable flight and high acceleration for an inherently unstable projectile.

CHARACTERISTICS OF EXTERNAL-JET PROPULSION

Figure-1 illustrates how fluid flow entering the diverging section of the projectile's interior is reflected rearward and channeled along the walls of the nozzle, which transfers momentum from the streamtube to the projectile.

Figure-1, Sphere-cone riding on blast of water

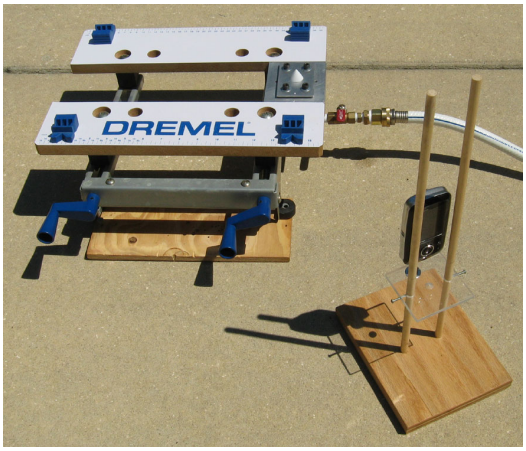

Figure-2, Apparatus for the blast experiment

Projectile stability and directional control is automatically achieved when the radial boundary layer forming the exit flow turns a projectile back into the direction of vertical flight as illustrated by Figure-1. In this image, flow exiting from the right side of the projectile rotates the sphere-cone into vertical flight therefore acting like an attitude control thruster. The alternating side-to-side thruster action described by Figure-1 occurs many times per second causing the projectile to ride on a narrow streamtube of water several meters into the air, demonstrating stable flight of an inherently unstable object. Figure-2 illustrates the test apparatus where an adjustable-height camera, water baster and test vehicle are imaged. This paper proposes a new design for highly efficient projectiles that ride on an external-jet of high velocity water or high power laser energy. Efficiency of externally blasted projectiles is greatly enhanced because the extra mass of propellant normally carried by standard rocket vehicles and spacecraft is totally eliminated.

TEST DESCRIPTION

Prior to launch a sphere-cone projectile sits directly above a 1.587 mm diameter hole that is allowed to emit a narrow jet of water. The projectile while it sits above the nozzle is not constrained in any manner during impact from below by the jet of water. Figure-3 and Figure-4 displays a prototype design where a jet of water is designed to “shoot” from a small hole on the top surface of the aluminum base structure into the base region or nozzle of the projectile. Figure-4 illustrates a sphere-cone projectile in the launch position just prior to launch. Launch is achieved by quickly turning the valve handle 90 degrees in the counter-clockwise (CCW) direction and then by quickly turning the handle in the opposite direction when the projectile is several meters above the launch pad.

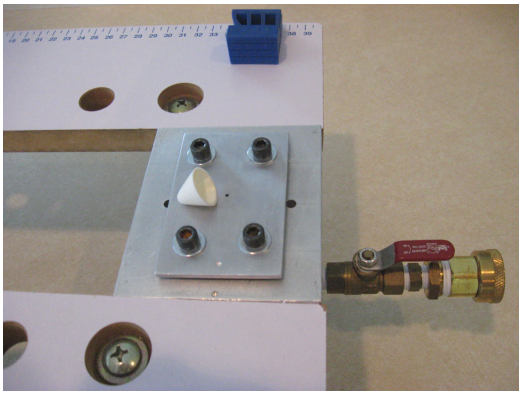

Figure-3, Prototype water-blast design

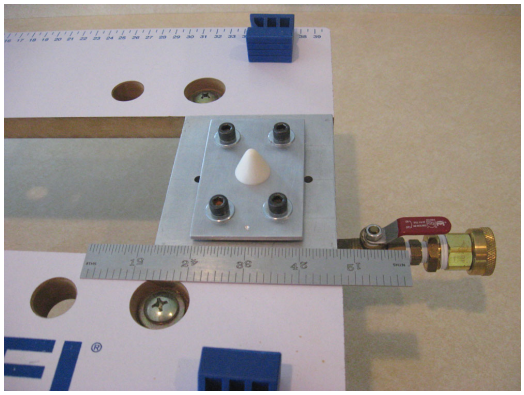

Figure-4, Projectile in launch position

Figure-5, Projectile position at t = 0.10 sec

Figure-6, Projectile position a t = 0.15 sec

RESULTS

Figure-5 and Figure-6 illustrate projectile flight position above the launch pad at 0.10 seconds and 0.15 seconds respectively after turning the fluid valve handle 90 degrees CCW. Using stop motion photography and applying appropriate scaling factors projectile velocity and altitude are 11.3 m/sec and 56.5 cm as illustrated in Figure-5 at t = 0.10 seconds. Using similar scaling techniques projectile velocity and altitude are 14.5 m/sec and 108.72 cm as illustrated in Figure-6 at t = 0.15 seconds. The sphere-cone projectile attained a maximum altitude of approximately 8.4 meters in 1.19 seconds for a total flight time of 2.83 seconds. Figure-7 displays time-sequenced video clips as the sphere-cone projectile is propelled skyward by a jet-blast of high velocity water. The **red** arrow identifies projectile position in each time-sequence image. Results derived from Figure-7 are displayed in TABLE I where measured verses theoretical projectile velocity and altitude are tabulated. Please note these velocity and altitude data must be verified because the stop motion photography resources used are approximate and must be refined using more advanced resources and techniques.

Figure-7, Sequence of movie images taken during external-jet propelled flight (0.15 to 1.19 sec).
See measured (V, Z) and theoretical (V, Z) in TABLE-1 then plotted (V, Z) in Figure-8 and Figure-9.

JET-BLAST FLIGHT ANALYSIS

Eqn. 1 describes the vertical motion of any projectile "blasted" by a jet of high velocity water. Newton's Second Law of Motion[2], states the rate of change of momentum, M**a** is proportional to the force, **F** applied in the same direction as the force. Where, force, **F** is due to a jet of high velocity water applied from below and external to the projectile.

$$F = Ma \tag{1}$$

Newton's *Second Law of motion* becomes the following when force, **F** is further defined to be composed of jet-blast thrust, **T** aerodynamic drag, **D** and projectile weight, **W**.

$$T - D - W = Ma \tag{2}$$

Further, aerodynamic drag, **D** and weight, **W** is is described by the following equations.

$$D = C_D \frac{1}{2} \rho_{air} {V_n}^2 \mathrm{A} \quad \text{and} \quad W = Mg \tag{3}$$

Force of the external fluid jet acting on the projectile is determined using the principal of conservation of linear momentum[3] as summarized by the following equation.

$F = 2MV\sin\left(\frac{\theta}{2}\right)$. Where, θ is the turning angle of the nozzle exit flow. (4)

After performing a little algebra, vertical acceleration, **a** velocity, **V** and altitude, **z** is determined using a finite difference procedure. The finite difference method used in this paper first uses Eqn. 5 during the thrusting phase of flight when the thrust force term is non-zero. Then, during the coasting phase of flight Eqn. 6 is used because the thrust force term is negligible when the projectile is out of effective range of the jet. Where, θ is now the flight angle of the projectile at liftoff.

$$a_{n+1} = \frac{F_n}{M} - \frac{C_D A \rho_{air} {V_n}^2}{2M} - g\sin\theta \qquad V_{n+1} = V_n + a_n \Delta T \qquad z_{n+1} = Z_n + V_n \Delta T \tag{5}$$

$$a_{n+1} = -\frac{C_D A \rho_{air} {V_n}^2}{2M} - g\sin\theta \qquad V_{n+1} = V_n + a_n \Delta T \qquad z_{n+1} = Z_n + V_n \Delta T \tag{6}$$

TABLE I, measured verses theoretical projectile velocity, altitude and acceleration

T (sec)	V (m/sec) **Measured**	V (m/sec) **Theoretical**	*z* (cm) **Measured**	*z* (cm) **Theoretical**	G's **Theoretical**
0.10	11.3	10.725	56.53	56.53	10.145
0.15	14.5	15.278	108.72	112.418	8.663
0.19	--	18.348	--	178.30	7.321
0.25	--	15.506	--	280.90	-4.315
0.50	--	8.528	--	573.80	-1.994
1.19	--	0.0	--	837.00	-1.0

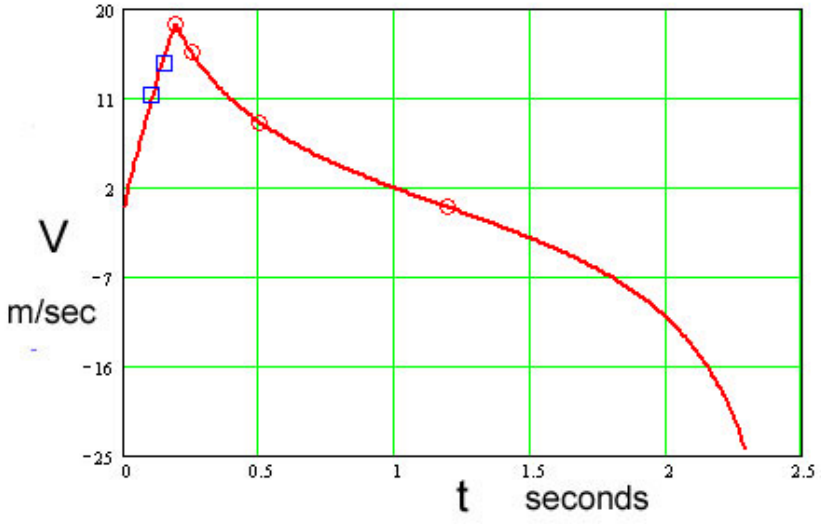

Figure-8, Measured projectile velocity (**blue squares**) verses theoretical results (**red circles/line**)

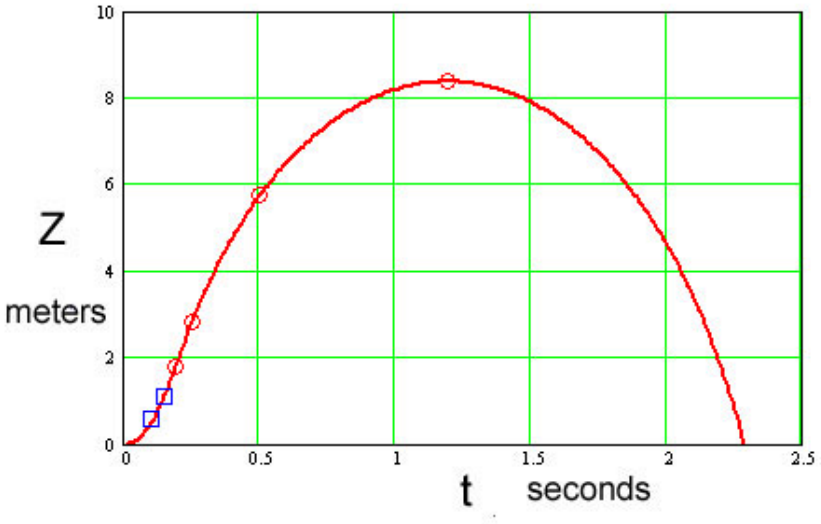

Figure-9, Measured projectile altitude (**blue squares**) verses theoretical results (**red circles/line**)

DRAG COEFFICIENT (C_D) PREDICTED USING VisualCFD[4]

VisualCFD™ quickly and easily determines axial drag coefficient (CX) using 3-D source panels to solve the frictionless Euler equations for subsonic compressible fluid flow up to Mach 0.80. A complete set of graphical tools such as velocity and pressure contour plots are provided to allow the user to visualize 3-D flow around the model. VisualCFD computes axial drag coefficient (CX) by integrating pressure forces acting parallel to the axis of the model. Normal force coefficient (CN) is determined by integrating pressure forces acting perpendicular to the axis of the model. Base drag is determined using a separate methodology not based on CFD methods using the venerable NASA TR R-100[5].

Ballistic tests were conducted using the jet-launcher illustrated in Figure-5 and Figure-6. This section summarizes aerodynamic results and validates **VisualCFD** for the prediction of drag coefficient C_D for subsonic flight of blunt sphere-cone projectiles. VisualCFD aerodynamic results and contour plots depicted in Figure-10 and Figure-11 display the value of C_D used in Eqn. 5. Where, projectile geometry is defined to have a spherical nose radius of 0.30 cm, total length of 1.35 cm and half angle of 30 degrees. Simply stated, VisualCFD predicts the axial drag coefficient is 0.515 and base drag is 0.129. VisualCFD was validated with great success using results from the experimented data compiled by Fluid Dynamic Drag[6]. Wind tunnel data from Fluid-Dynamic Drag, interpolated as illustrated in Figure-12, states the axial drag force coefficient for 30-degree half-angle cones should be 0.585 compared to the VisualCFD, C_D result of 0.515. This "engineering" comparison indicates wind tunnel results and VisualCFD results for subsonic drag coefficient ($C_D = \mathrm{CX}$) of a sphere-cone are within 12%. The predicted VisualCFD value for drag coefficient, C_D was inserted into the flight analysis described in the **JET-BLAST FLIGHT ANALYSIS** section. Figure-8 and Figure-9 document results from the flight analysis where velocity verses time and altitude verses time are plotted. Where, it is seen the measured flight data (red squares) compare well to theoretical flight analysis results determined by a **MathCAD** finite difference solution.

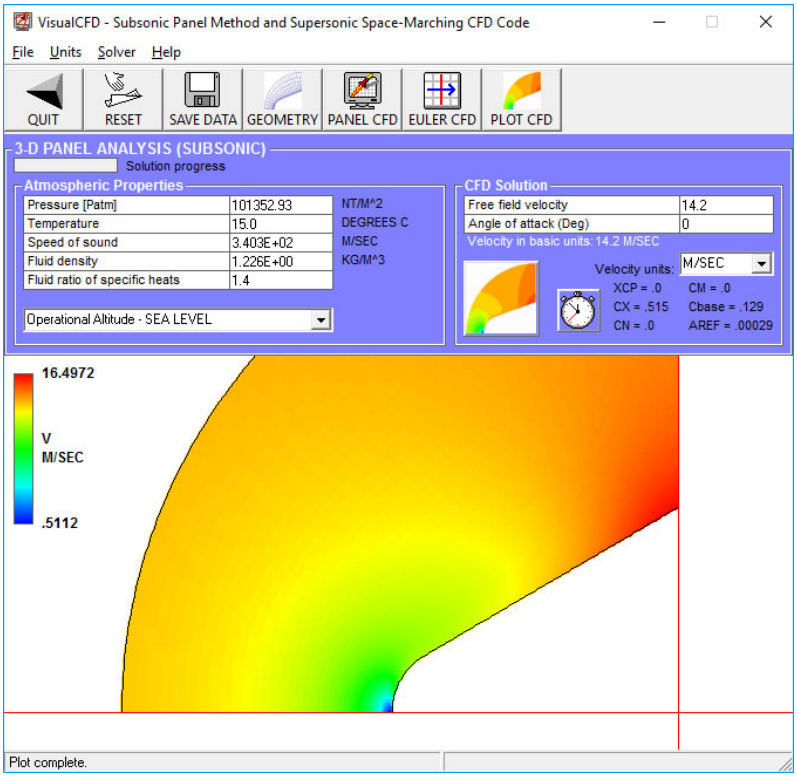

Figure-10, VisualCFD™ velocity contour plot. Cd = 0.515 and Cdbase = 0.129

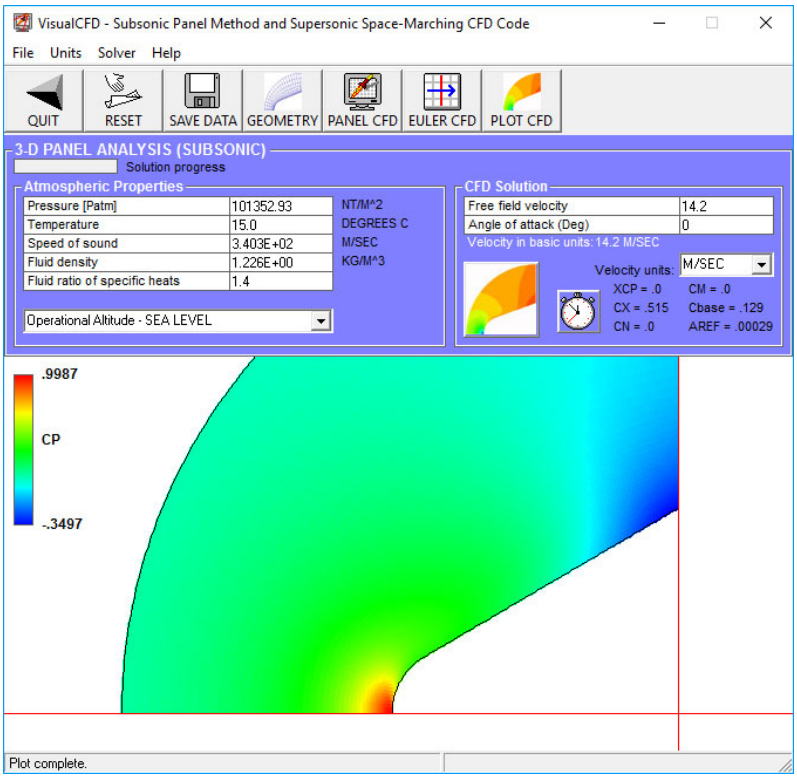

Figure-11, VisualCFD™ pressure coefficient contour plot

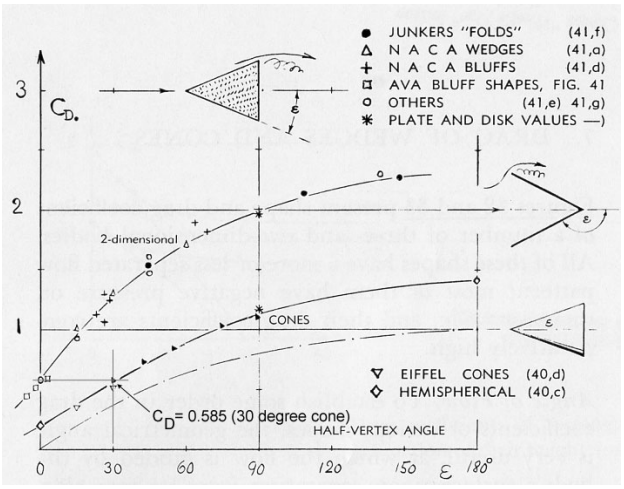

Figure-12, Fluid-Dynamic Drag, page 3-18, Figure-34 for drag of 3D cones

Cd VALIDATION FOR THE JET-BLAST FLIGHT ANALYSIS

The AeroRocket subsonic wind tunnel was used to verify that the drag coefficient (Cd) predicted by VisualCFD and verified by Fluid-Dynamic Drag would allow the Jet-Blast Flight Analysis to provide accurate altitude (Z) and velocity (V) results verses time.

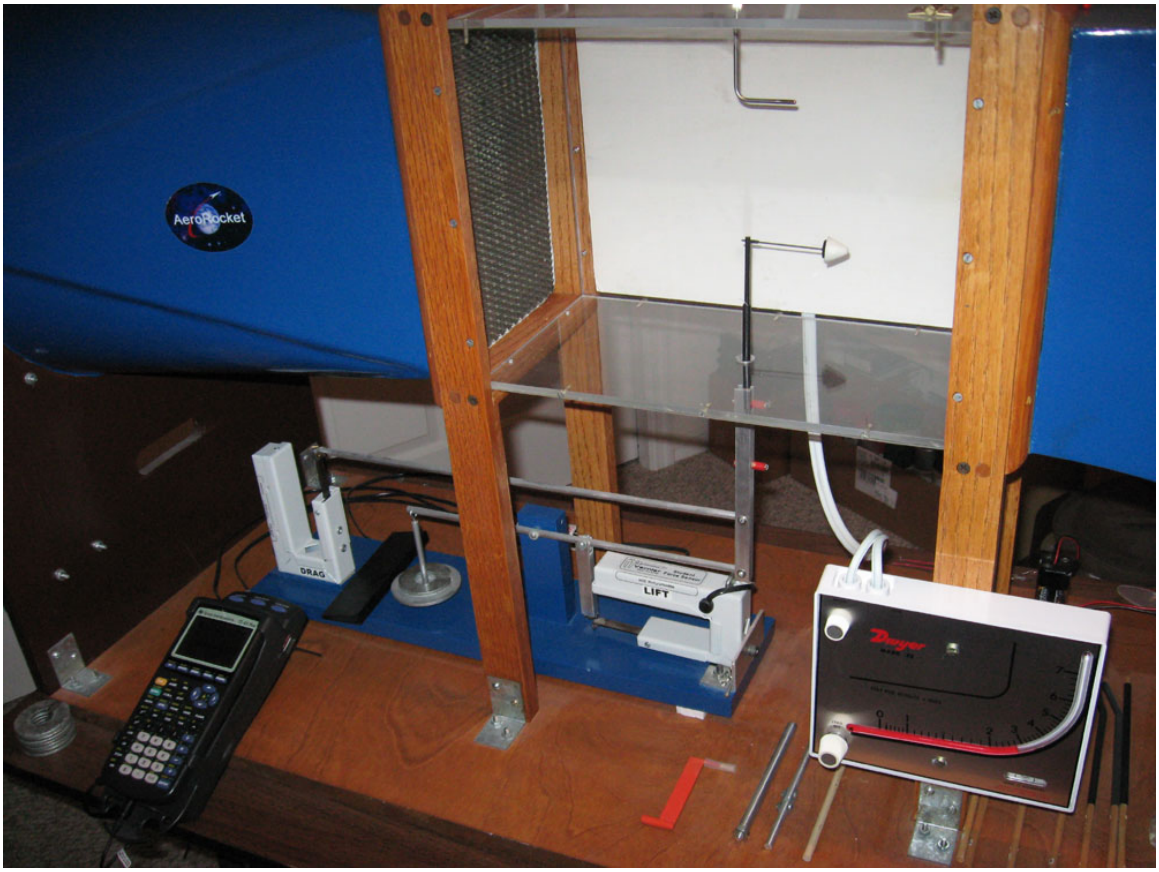

Figure-13, AeroRocket wind tunnel used to validate the Cd used in the flight analysis

Figure-13 illustrates how the AeroRocket wind tunnel was used to measure the drag coefficient of the jet-blasted sphere-cone projectile. Table II compares the C_D determined by the AeroRocket wind tunnel, VisualCFD and Fluid Dynamic Drag. The result, $C_D = 0.515$ predicted by VisualCFD was used in the flight analysis based on the dimensional data and physical properties presented in Table II. Notice the excellent agreement for the value of C_D predicted by the three methods described in Table II.

TABLE II, Measured and theoretical drag coefficient of 3D cone with the specified dimensions

	AeroRocket Wind Tunnel	**VisualCFD**	**Fluid-Dynamic Drag**
Cd	0.534	0.515	0.585
U_∞	14.2 $\frac{m}{sec}$	14.2 $\frac{m}{sec}$	Free stream velocity
ρ_∞	1.186 $\frac{kg}{m^3}$	1.186 $\frac{kg}{m^3}$	Air mass density
Re	17,916	17,916	Reynolds number
D_{max}	1.9 cm	1.9 cm	Model maximum diameter
S_{max}	2.835 cm^2	2.835 cm^2	Model reference area

PHOTONIC PROPULSION MOMENTUM EXCHANGE ANALOGY

A lightsail uses the momentum of reflected and absorbed photons to generate thrust by the transfer of momentum from the momentum of the incident laser beam into the forward momentum of the spacecraft. Please see Figure-14 illustrating how a lightsail can use photonic propulsion to travel at speeds up to 20 percent of the speed of light. Using a methodology similar to the fluid dynamics discussed for an external-jet, the principal of conservation of linear momentum can be used to determine the force of the laser beam acting on the lightsail. If the lightsail is flat and highly reflective it is reasonable to assume the angle of reflected light is equal to the angle of the incident light beam.

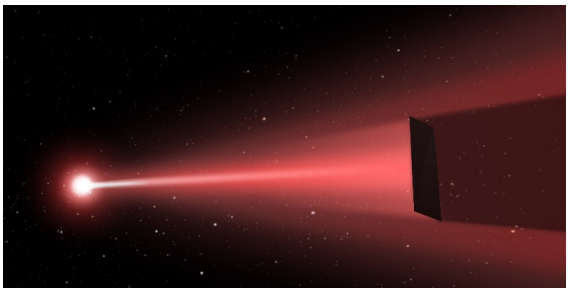

Figure-14, Lightsail using photonic propulsion traveling to Alpha Centauri at 0.20c

The resulting laser force in a direction normal to the lightsail is the vector resultant of the incident and reflected light beams. Therefore, the vector sum of the transferred momentum of the incident and reflected light beams is described by the following relationship for the laser force[7], F_n acting normal to the lightsail.

$$F_n = F_s sin\theta + F_i sin\theta = 2F_i sin\theta = \frac{2SA}{c} sin^2\theta \quad (7)$$

Where, S is laser-light flux (W/m^2), A is lightsail area, c is the speed of light and θ is the angle of the incident and reflected light beams having momentum, p.

And momentum[8], p is a function of Planck constant, h and wavelength of light, λ.

$$p = h/\lambda \quad (8)$$

Finally, this paper proposes that a design analogy exists between the fluid-jet force expressed by Eqn. 4 and the force due to momentum transfer from a laser beam to the lightsail expressed by Eqn. 7. Please see an interesting video describing the technology behind Photonic Propulsion presented by the NASA engineer, Philip Lubin.

References

[1]Philip. Lubin, "A Roadmap to Interstellar Flight", JBIS (2015), Using light-blast for relativistic speeds

[2]Roger R Bate, Donald D Mueller, Jerry White, *Fundamentals of Astrodynamics* (Dover, NY, 1971)

[3]F. M. White, *Fluid Mechanics*, (McGraw-Hill, New York, 2010), Conservation of linear momentum

[4]John Cipolla. VisualCFD™, Subsonic Panel Method and Supersonic Space-Marching CFD Code

[5]William E. Stoney, "COLLECTION OF ZERO-LIFT DRAG DATA ON BODIES OF REVOLUTION FROM FREE-FLIGHT INVESTIGATIONS", NASA TR R-100 (March 30, 1962)

[6]S. F. Hoerner, *Fluid-Dynamic Drag*, (Published by author, 1965)

[7]R. Humble, G. Henry and W. Larson, *Space Propulsion Analysis and Design* (McGraw-Hill, NY, 1995)

[8]D. Halliday, R. Resnick, J. Walker, *Fundamentals of Physics-7th Edition*, (John Wiley & Sons, New Jersey, 2005